DEMONSTRATION OF EXPONENTIAL GROWTH AND SATURATION AT VUV WAVELENGTHS AT THE TTF FREE-ELECTRON LASER

P. Castro*, DESY, Hamburg

Abstract

We present experimental evidence that the free-electron laser (FEL) at the TESLA Test Facility has reached the maximum power gain of 10^7 in the vacuum ultraviolet (VUV) region at wavelengths between 80 and 120 nm. At saturation the FEL emits short pulses with GW peak power and a high degree of transverse coherence. The radiation pulse length can be adjusted between 30 fs and 100 fs. Radiation spectra and fluctuation properties agree with the theory of high gain, single-pass free-electron lasers starting from shot noise. Both FEL results and related accelerator physics issues studied at TTF will be presented.

1 INTRODUCTION

The experimental results presented in this paper have been achieved at the TESLA Test Facility (TTF) Free-Electron Laser [1] at DESY. The TESLA (TeV-Energy Superconducting Linear Accelerator) collaboration consists of 44 institutes from 10 countries and aims at the construction of a 500 GeV (center-of-mass) e^+/e^- linear collider with an integrated X-ray laser facility [2].

Since the first lasing observed at the TTF [3] the performance of the Self-Amplified Spontaneous Emission (SASE) FEL has been steadily improved. By varying the energy of the linear accelerator, full wavelength tunability in a wide range from 80 to 180 nm [4] has been demonstrated, as depicted in Figure 1. Further work has been focused on the range from 80 nm to 120 nm by request of first scientific users. Recently, saturation has been achieved in this entire wavelength range.

2 LAYOUT OF THE TTF FEL

The present TTF layout (phase 1) is shown in Figure 2. The main parameters for FEL operation are given in Table 1.

The injector is based on a laser-driven photocathode installed in a $1\frac{1}{2}$-cell radio-frequency (rf) cavity operating at 1.3 GHz [8] with a peak accelerating electric field of 37 MV/m on the photocathode. At the exit of the cavity the electron energy is 4 MeV. The Cs_2Te cathode [9] is illuminated by a train of UV laser pulses generated in a mode-locked solid-state laser system [10] synchronized with the rf. It generates bunch charges of several nC at up to 2.25 MHz repetition rate [11]. The UV pulse length measured with a streak camera is $\sigma_t = 7.1 \pm 0.6$ ps . The operational parameters of this photoinjector required by the FEL operation are presented in this conference [12].

* The author list is given in ref. [5]

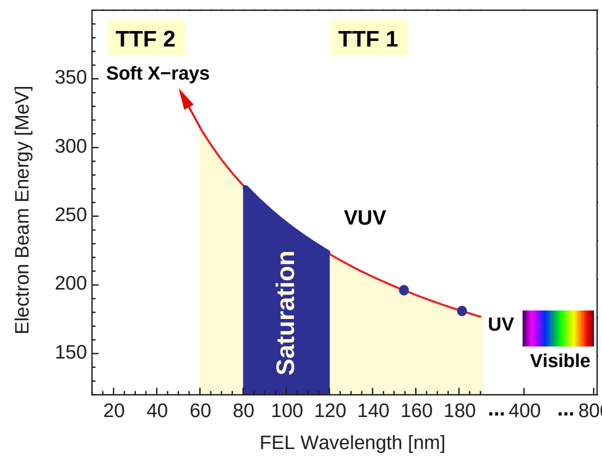

Figure 1: VUV wavelength range within which lasing has been obtained at the TTF FEL, phase 1 (TTF1). The wavelength was tuned by changing the electron beam energy. The individual dots outside the range in which saturation has been achieved represent an FEL gain of typically > 1000 demonstrated in an earlier stage of the experiment [4]. After a linac upgrade to electron beam energies of up to 1 GeV (TTF 2), the FEL will enter the soft X-ray region [6].

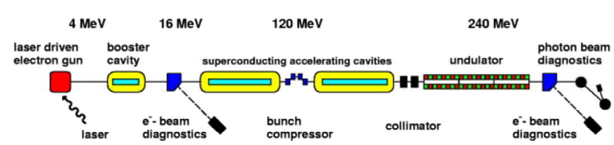

Figure 2: Schematic layout of the TESLA Test Facility Linac. The total length is about 120 m.

The gun section is followed by a 9-cell superconducting cavity, boosting the energy to 16 MeV. Two 12.2 m long accelerating modules each containing eight 9-cell superconducting niobium cavities [7] provide a beam energy of up to 300 MeV. In the first module the electrons are accelerated on the slope of the rf wave to impress a position-dependent energy distribution within the bunch, the front electrons receiving lower energy gain than the tail electrons. In the following magnetic chicane [13] the front particles move on a longer trajectory than the tail particles. Thereby the bunch lengths can be reduced by a factor of five and high peak currents needed for the FEL can be achieved.

The undulator is a permanent magnet device [14] with a 12 mm gap. The undulator system is subdivided into three segments, each 4.5 m long and containing 10 permanent-magnet quadrupoles with alternating gradients, which are superimposed on the periodic undulator field.

Electrons:	
beam energy	$220 - 270$ MeV
bunch charge	2.7-3.3 nC
charge in lasing part of bunch	0.1-0.3 nC
peak current	1.3 ± 0.3 kA
rms energy spread	150 ± 50 keV
rms normalized emittance	$(6 \pm 2)\pi$ mm·mrad
Undulator:	
undulator period λ_u	27.3 mm
undulator peak field	0.47 T
average beta-function	1.2 m
magnetic length of undulator	13.5 m
Photons:	
radiation wavelength	80-120 nm
energy in the radiation pulse	$30 - 100$ μJ
FWHM radiation pulse duration	$50 - 200$ fs
radiation peak power level	1 GW
spectral width (FWHM)	1%
spot size at undu. exit (FWHM)	250 μm
rad. angular divergence (FWHM)	260 μrad

Table 1: Main parameters of the TESLA Test Facility for FEL experiments (TTF FEL, phase 1)

3 EXPERIMENTAL RESULTS

For a characterization of the FEL process, the energy of the radiation as well as its spectral characteristics and angular distribution have been measured.

3.1 Exponential Growth

The average energy of the radiation pulse measured as a function of the active undulator length is shown in Figure 3. The active length is defined as the distance over which the electron beam and the photon beam overlap. The wavelength for this measurement was chosen at 98 nm. Figure 3 clearly exhibits the exponential growth of FEL power with the undulator length. The almost constant level of radiation energy observed for an active undulator length of less than 5 m does not imply that there is no FEL gain in this part of the undulator. In contrast, this is due to the fact that in the first few meters of the undulator, the FEL radiation stays below the energy of spontaneous radiation accumulated over the entire undulator of about 2.5 nJ for the entire electron bunch. By providing a good overlap of the two beams over an increasing length of the undulator, the FEL amplification is gradually switched on and the radiation energy rises exponentially until a plateau is reached at a level of 30 to 100 μJ, depending on the accelerator tuning. We conclude that the FEL gain is about 10^7 in terms of effective power of shot noise. The measured power growth is also in agreement with the theoretical expectation. The solid curve in Figure 3 represents a three-dimensional numerical Self-Amplified Spontaneous Emission (SASE) simulation [15] using the electron beam and undulator parameters of Table 1 which were experimentally verified.

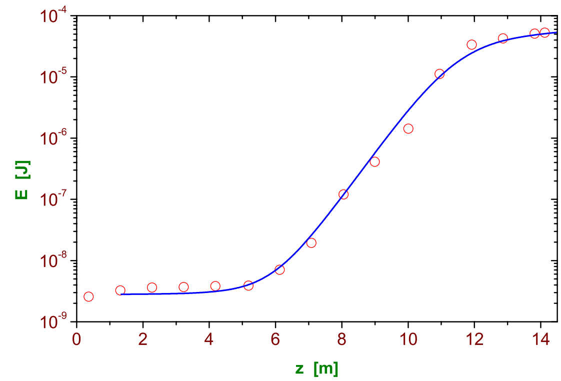

Figure 3: Average energy in the radiation pulse as a function of the active undulator length. Measurments are shown with circles. Results of numerical simulations with the code FAST [16] using parameters of Table 1 are shown with a solid line.

3.2 Spectral Measurements

The pulse duration is a very important parameter but presently not accessible to direct measurement in the time domain. The FWHM spectral width $\Delta\omega$ of each peak in the single shot spectrum is related to the approximate radiation pulse length by $\tau_{\rm rad} \simeq 2\pi/\Delta\omega$. Measurements of the spectral distribution taken for two bunch compressor settings are presented in Figure 4. The radiation pulse length corresponds to $\tau_{\rm rad} \simeq 50$ fs (top) and $\simeq 100$ fs (bottom). The single shot spectra show an ensemble of a few peaks which reflect the number of longitudinal modes in the radiation pulse [17], as it is expected for SASE FEL radiation starting from shot noise.

3.3 Random Fluctuations

The fluctuations seen in the single spectra of Figure 4 are not due to unstable operation of the accelerator but are inherent to the SASE process. Shot noise in the electron beam causes fluctuations of the beam density, which are random in time and space [19]. As a result, the radiation produced by such a beam has random amplitudes and phases in time and space and can be described in terms of statistical optics. A detailed study of spectral fluctuations and of pulse-to-pulse fluctuations measured at different pulse length is presented in [5].

3.4 Transverse Coherence

A crucial feature is the transverse coherence of the FEL radiation [20]. Figure 5 shows two diffraction patterns of the FEL radiation measured in a distance of 3 m behind a double slit and two crossed slits (see pictographs), respectively. The remarkably high fringe visibility is a proof of the high degree of transverse coherence. The transverse coherence of the FEL radiation illustrated by the diffraction patterns has been corroborated by measurements of the

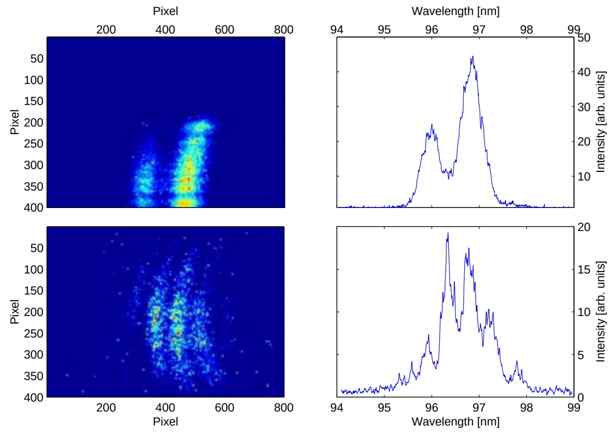

Figure 4: Spectra from short (top) and long (bottom) FEL pulses. On the left hand side, the CCD image of the dispersed FEL radiation in the exit plane of the monochromator is shown in a false color code. The dispersive direction is in the horizontal. On the right hand side, the spectra are evaluated quantitatively along the horizontal center line of the CCD image. It is seen that the number of optical modes are different: For our short pulse setting (top) there are, in average, 2.6 modes, in the long pulse setting (bottom) there are 6 modes in average.

opening angle of the radiation [15].

3.5 Peak Brilliance

With a number of $2 \cdot 10^{13}$ photons per pulse, a pulse length of 50 fs and the full transverse coherence, the peak brilliance is $2 \cdot 10^{28}$ photons/(s $\cdot$ mrad^2 $\cdot$ mm^2 $\cdot$ (0.1% bandwidth)), eight orders of magnitude higher than at third generation synchrotron radiation sources The peak radiation power is about a gigawatt.

4 CONCLUSION AND OUTLOOK

A new generation of radiation sources for VUV radiation at wavelengths in the 100 nm range has become available exceeding the peak brilliance of other existing sources by several orders of magnitude. Due to the basic underlying principle, full wavelength tunability and adjustable pulse lengths below 100 fs are possible and have been demonstrated.

The device will be upgraded to a user facility for soft X-rays available for scientific users starting in 2004. The demonstrated technology is also suitable to realize a X-ray laser user facility for Ångström wavelengths [21, 22, 2], such as proposed within the TESLA project.

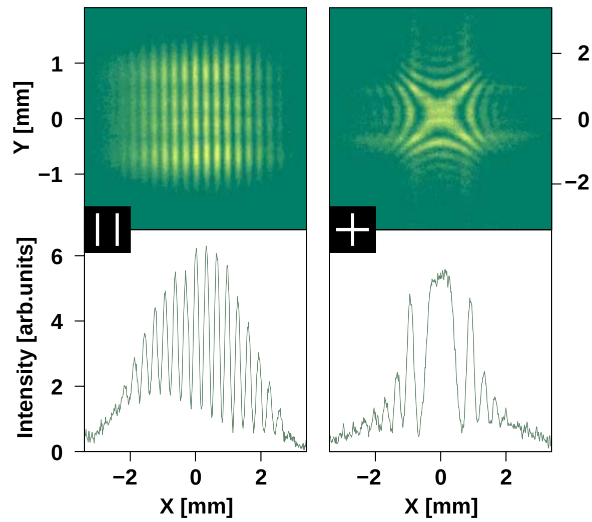

Figure 5: Diffraction patterns of two different slit arrangements (see pictographs) illustrating the transverse coherence of the FEL radiation. On the **left:** double slit, each slit 2 mm (vert) $\times$ 200μm (horiz.), horizontal slit separation 1 mm. On the **right:** crossed slits, each slit 4 mm$\times$ 100μm. The slits are located 12 m behind the exit of the undulator. The images have been recorded with a gated CCD camera viewing a Ce:YAG fluorescent screen 3 m behind the slits. They have been taken as a sum of a few consecutive FEL pulses with a wavelength of 95 nm. The lower part of both images depicts a horizontal cut through the centre of the respective diffraction pattern.

5 REFERENCES

[1] W. Brefeld et al., Nucl. Instr. and Meth. **A393**, 119 (1997).

[2] F. Richard et al. (eds.),TESLA Technical Design Report, DESY2001-011, and http://tesla.desy.de.

[3] J. Andruszkow et al., Phys. Rev. Lett. **85** 3825 (2000).

[4] J. Rossbach et al., Nucl. Instr. and Meth. **A475,** 13 (2001)

[5] V. Ayvazyan et al., accepted for publication in the Euro. Phys. Journal Sec.D, 2002.

[6] J. Rossbach, Nucl. Instr. and Meth. **A 375,** 269 (1996).

[7] H. Weise, Proc. 1998 Linac Conf. Chicago, 674-678 (1998).

[8] J.-P. Carneiro, et al., Proc. of the PAC 1999, New York.

[9] D. Sertore et al., Nucl. Instr. and Meth. **A445,** 422 (2000).

[10] I. Will et al. Proc. of the 1999 FEL Conf., Hamburg.

[11] S. Schreiber et al. Nucl. Instr. and Meth. **A445,** 427 (2000).

[12] S. Schreiber, this conference procedings (TUPRI052).

[13] T. Limberg et al., Nucl. Instr. and Meth. **A375,** 322 (1996).

[14] Y. M. Nikitina et al. Nucl. Instr. and Meth. **A375,** 325 (1996).

[15] V. Ayvazyan et al., Phys. Rev. Lett.**88,** No.10 (2002).

[16] E.L. Saldin et al., Nucl. Instr. and Meth. **A429**, 233 (1999).

[17] E.L. Saldin et al., Opt. Commun. **148**, 383 (1998).

[18] R. Bonifacio et al., Opt. Commun. **50,** 373 (1984).

[19] R. Bonifacio et al., Phys. Rev. Lett. **73,** 70 (1994)

[20] L. Kipp et al., Nature **414**, 184 (2001)

[21] H. Winick et al., Proc. PAC Washington and SLAC-PUB-6185, (1993).

[22] R. Brinkmann et al., Nucl. Instr. and Meth. **A 393,** 86-92 (1997).